Original Article

Institution of MECHANICAL ENGINEERS
Journal of AEROSPACE ENGINEERING

Proc IMechE Part G:
J Aerospace Engineering
2023, Vol. 237(11) 2665–2676

DOI: 10.1177/09544100231156638
journals.sagepub.com/home/pig
Sage

Adaptive second order sliding mode guidance law for missile-target interception with fuzzy logic system

Handan Gürsoy-Demir[1,2] and Mehmet Önder Efe[3]

Abstract

This paper presents the design of a 3D missile guidance law based on a second order sliding mode control technique employing an adaptive tuning law and a fuzzy gain scheduling. At the outset, the super-twisting sliding mode guidance law is obtained to overcome the chattering phenomenon. Then, without the knowledge about the bounds of disturbances, an adaptive law is used to determine the control gains. The results are enhanced using a fuzzy module that provides the controller parameters according to a set of linguistic rules. Finally, a comparative set of simulation results are given. To verify the performance and effectiveness of the proposed guidance law, we compare the performances of the traditional sliding mode (SM) guidance law, the traditional super-twisting sliding mode (STWSM) guidance law, the adaptive super-twisting sliding mode (ASTWSM) guidance law and the adaptive fuzzy super-twisting, sliding mode (AFSTWSM) guidance law. The simulation scenarios consider fundamental target movements. The results demonstrate that the proposed adaptive guidance laws display better performance in terms of miss distance, intercept time, and final closing velocity compared the alternatives considered in this study.

Keywords

Guidance laws, second-order sliding mode control, super-twisting algorithm, adaptive control, fuzzy logic control

Date received: 30 November 2021; revised: 22 October 2022; accepted: 23 January 2023

Introduction

During the past few decades, guidance law design for missile systems has been studied by many researchers and engineers. There are well-known guidance approaches in the field of missile guidance and control, such as Proportional Navigation (PN), True Proportional Navigation (TPN), Optimal Guidance Law (OGL) etc. However, under demanding operational conditions and constraints, such traditional guidance solutions have become either impractical or insufficient in terms of performance. Thus, in order to meet the real-time requirements for missile-target interception, a number of robust control methods have been employed in the guidance systems, such as sliding mode (SM) control[1–4], optimal control[5], and $\mathcal{H}_\infty$ control.[6]

Because of its prominent features, such as robustness and bandwidth, the traditional Sliding Mode Control (SMC) is successfully employed in designing missile guidance systems.[1,3] Zhang et al.[1] propose a sliding mode guidance law by taking into account the terminal impact angle constraint. Using the SMC algorithm, Shin et al.[3] present a novel 3D guidance law for the interception of maneuvering targets. On the other hand, it is well known that the SMC framework suffers from the chattering phenomenon arising due to the discontinuous switching term. To alleviate the disadvantages of the discontinuity in the control law, one remedy is to use a saturation function introducing a boundary layer around the sliding subspace and giving concessions from the performance. The second remedy is the use of a high-order SMC approach, which has been studied extensively in the recent years and a widely used variant of it is called super-twisting SMC.[7–9]

The super-twisting SMC method is one of the second-order SMC methods and it is known for its robustness and eliminated chattering.[9–11] Zhao et al.[10] design the controller by using this method for a tethered space robot. In,[11] by utilizing a cascaded inner-outer loop structure, a super-twisting SMC is presented for a quadrotor. However, if the upper bounds of the disturbances and uncertainties are not known, they may be overestimated and the chattering can be further provoked. In order to

[1] Graduate School of Science and Engineering, Hacettepe University, Ankara, Türkiye
[2] Department of Computer Engineering, Iskenderun Technical University, Hatay, Türkiye
[3] Department of Computer Engineering, Hacettepe University, Ankara, Türkiye

Corresponding author:
Handan Gürsoy-Demir, Department of Computer Engineering, Iskenderun Technical University, Hatay, Türkiye.
Emails: handan.gursoy@iste.edu.tr; handangrsy@gmail.com

overcome this problem, an adaptive law is developed.[12–14] Thus, thanks to the adaptive law, it is not necessary to have the upper bound information of the disturbances and uncertainties. In,[13] the controller based on the super-twisting SMC method with an adaptive law is proposed for the 6 degrees-of-freedom (dof) nonlinear unmanned aerial vehicle and also two separate controllers are designed by taking account into the equations of motion. An adaptive super-twisting algorithm is proposed in[15] for a microgyroscope under unknown model uncertainties and external disturbances.

For many years, numerous studies in which fuzzy logic has been used together with the SMC method have been reported in the literature. Since the fuzzy logic control method is a rule-based algorithm, determining different gains for different partitions of the input space is a remedy to the problem of very large/small gain selection. In,[16] an adaptive fuzzy gain-scheduling SMC scheme is presented for unmanned quadrotor vehicle and the goal is to solve the problem of attitude regulation. In,[17] a new controller, which is designed by utilizing an adaptive fuzzy high-order super-twisting SMC method, is proposed to accomplish certain trajectory tracking for a robotic manipulator under external disturbances and unknown uncertainties of the system. In,[18] for spacecraft attitude tracking for space debris removal, an adaptive fuzzy SMC approach is developed under external disturbances and uncertainties.

In,[14] a nonsingular adaptive super-twisting guidance is proposed for missile-target planar engagement geometry subject to impact angle constraint. In,[12] a nonsingular fast terminal sliding mode guidance law is developed for the targets. The approach considers maneuvering motion and impact angle constraints and addresses the singularity problem of the terminal SMC scheme. Moreover, the same work proposes a fast terminal sliding mode dynamics with finite-time convergence with an adaptive smooth super-twisting algorithm. Xu et al.[19] present a novel guidance law based on the composite nonsingular fast terminal sliding mode and adaptive super-twisting algorithm. However, the work reported by Xu et al.[19] considers the motion of the missile and target in the pitch plane. Using the SMC method and a fuzzy logic system, Li et al.[20] propose a novel guidance law under various terminal constraints, which are miss distance, impact angle, and acceleration for the missile-target interception. Another remarkable application of the fuzzy SMC method is reported by Elhalwagy et al.[21] where a guidance law for the trajectory control of a command guidance system is considered. The developed guidance law in comparison with each of the studies listed above was examined. Contrary to the previously proposed guidance laws in,[14,19] the presented guidance law is based on three-dimensional geometry in this paper. Unlike studies in the literature,[12,14,19,20] two sliding manifolds are determined. In addition, the structure established using the super twisting sliding mode, dynamic adaptive law, and fuzzy gain-scheduling are combined differently from its counterparts.

In this paper, a novel adaptive super-twisting sliding mode (ASTWSM) based guidance law with an auxiliary fuzzy logic system is presented. The efficacy of the approach is shown on a missile-target interception problem in three-dimensional geometry. The main contributions and features of the proposed guidance law can be summarized as below.

1. At the outset, sliding manifolds are designed separately for the axes to be considered, thus preventing any loss of information.
2. Then, the guidance law is developed on the basis of sliding mode and super-twisting sliding mode control methods. This eliminates the adverse effects of the chattering phenomenon.
3. Moreover, an adaptive dynamic system is used to handle the overestimation of the gain. Thus, thanks to the adaptive law, the parameters are obtained without the need for upper-bound knowledge of the disturbances. The stability properties of the proposed novel guidance law are investigated by using the Lyapunov stability framework.
4. Finally, in order to find an enhanced set of parameters of the sliding manifold, a fuzzy logic system has been utilized.

Comparative results with traditional methods are presented to prove the superior performance of the proposed adaptive guidance scheme. The results of the four different methods, namely, SM, super-twisting sliding mode (STWSM), ASTWSM, and adaptive fuzzy super-twisting sliding mode (AFSTWSM), are discussed and the numerical results emphasize that the developed guidance law displays better performance in terms of miss distance, intercept time, and final closing velocity than the alternatives studied here.

This work advances the subject area toward adaptive, fuzzy, and stable solutions for missile-target interception problem in particular and precise air defense systems in general. The designed system structure differs from the existing literature by removing the necessity to bound information for disturbances, domain-specific gain scheduling via fuzzy logic, and chattering-free implementation of SMC.

This paper is organized as follows: The second section presents the background of the problem with necessary analytical facts. The traditional STWSM guidance law, analytical details of the proposed approach and the stability analysis are given in the third section. The fourth section discusses the numerical simulations and comparative results supporting the effectiveness and superiority of the proposed approach. The last part of the paper is devoted to the concluding remarks.

Background

Problem formulation

In this subsection, the mathematical model of the guidance system for the missile-target interception problem is described. In Figure 1, the relative motion between the

missile and the target is depicted. The missile is denoted by M and the target is denoted by T. In this paper, in the three-dimensional engagement geometry, six dof mathematical model of the missile is considered and the equations of the relative motion of the missile and the target are given in (1)–(3).[22,23]

$$\ddot{R} - R\dot{\phi}^2 - R\dot{\theta}^2\cos^2\phi = a_{TR} - a_{MR} \tag{1}$$

$$R\ddot{\phi} + 2\dot{R}\dot{\phi} + R\dot{\theta}^2\sin\phi\,\cos\phi = a_{T\phi} - a_{M\phi} \tag{2}$$

$$R\ddot{\theta}\,\cos\,\phi + 2\dot{R}\dot{\theta}\,\cos\,\phi - 2R\dot{\phi}\dot{\theta}\,\sin\,\phi = a_{M\theta} - a_{T\theta} \tag{3}$$

where $R, \dot{R}, \theta, \phi$ represent the relative distance, the relative velocity, the elevation angle, and the azimuth angle of the line of sight (LOS), respectively. In addition, a_{TR}, $a_{T\theta}$, $a_{T\phi}$ are the components of the target acceleration and a_{MR}, $a_{M\theta}$, $a_{M\phi}$ denote the components of the missile acceleration.

Rewriting (2)–(3) by defining $x_1 = \phi, x_2 = \dot{\phi}, x_3 = \theta, x_4 = \dot{\theta}$, the state space representation is obtained as below

$$\begin{aligned}
\dot{x}_1 &= x_2 \\
\dot{x}_2 &= -\frac{2\dot{R}}{R}x_2 - x_4^2\sin x_1\cos x_1 - \frac{a_{M\phi}}{R} + \frac{a_{T\phi}}{R} \\
\dot{x}_3 &= x_4 \\
\dot{x}_4 &= -\frac{2\dot{R}}{R}x_4 + 2x_4x_2\tan x_1 + \frac{a_{M\theta}}{R\cos x_1} - \frac{a_{T\theta}}{R\cos x_1}
\end{aligned} \tag{4}$$

The control input vector of the above model is $u := [a_{M\phi}\ \ a_{M\theta}]^T$.

Mathematical preliminaries

Lemma 1. Let $L_j \in \mathbb{R}$ for $j = 1, 2, \ldots, n$. The inequality

$$(|L_1| + |L_2| + \cdots + |L_n|)^q \le |L_1|^q + |L_2|^q + \cdots + |L_n|^q \tag{5}$$

is satisfied for $0 < q < 1$.[24]

Lemma 2. Let V be a positive definite Lyapunov function. There exist real numbers $\tau > 0$ and $0 < \sigma < 1$, such that $\dot{V}(t) \le -\tau V^{\sigma}(t)$. Then, V converges to zero in finite time. The settling time is given as

$$t_f \le t_0 + \frac{2V^{1-\sigma}(t_0)}{\tau(1-\sigma)} \tag{6}$$

where t_0 stands for the initial time.[25]

Assumption 1. It is assumed that $d(t)$ is the total disturbance acting on the system and the $\dot{d}(t)$ is bounded, that is

$$\left|\dot{d}(t)\right| \le \delta_f < \infty \tag{7}$$

where δ_f is the finite yet unknown bound of $d(t)$.

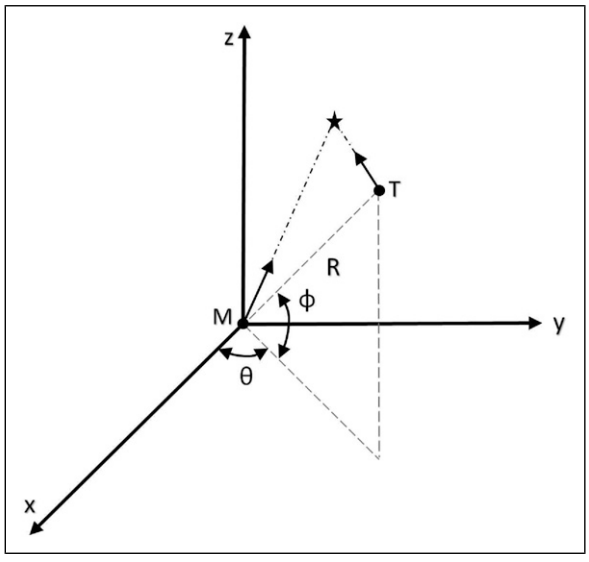

Figure 1. Missile-Target engagement geometry.

Design of the guidance law

Super-twisting sliding mode guidance law design

Considering the system dynamics given by (4), the sliding manifolds are defined as follows

$$s_1 := x_2 + k_1|x_1|^{\rho}\mathrm{sgn}(x_1) \tag{8}$$

$$s_2 := x_4 + k_2|x_3|^{\rho}\mathrm{sgn}(x_3) \tag{9}$$

where k_1, k_2 are positive constants, ρ is a positive constant satisfying $0.5 < \rho < 1$, and the vector of sliding manifolds is $s := [s_1\ \ s_2]^T$.

The elements of the control signal $u := [a_{M\phi}\ \ a_{M\theta}]^T$ are composed of two terms, namely, the equivalent control (u_{eq}) and the super-twisting control (u_{stw}) as given below

$$u = u_{eq} + u_{stw} \tag{10}$$

The equivalent control is obtained by setting $\dot{s} = 0$ and solving for the control term. The super-twisting control term in (10) is given as in

$$\begin{aligned}
u_{stw} &:= -\alpha|s|^{\frac{1}{2}}\mathrm{sgn}(s) + \upsilon \\
\dot{\upsilon} &= -\frac{\beta}{2}\,\mathrm{sgn}(s)
\end{aligned} \tag{11}$$

where $\alpha > 0$ and $\beta > 0$ are the controller gains.

Design of the adaptive super-twisting sliding mode guidance law

The adaptive super-twisting sliding mode guidance law for the system in (4) is proposed in this subsection. The adaptive law is utilized to obtain approximately the unknown control gains of the super-twisting controller. Thanks to the adaptive law, the chattering phenomenon is suppressed without the need for an upper bound information of the disturbance. Moreover, the control gains

of the super-twisting SMC are able to adapt to uncertainties online.

The control gains given in (11) can be calculated by using the following adaptive algorithm

$$\dot{\alpha} = \begin{cases} w_1\sqrt{\frac{\gamma_1}{2}}\ \mathrm{sgn}(|s| - \zeta) & : \alpha \geq \alpha_m \\ \eta & : \alpha < \alpha_m \end{cases} \qquad \beta = 2\ \kappa\ \alpha \tag{12}$$

where $w_1, \gamma_1, \zeta, \eta, \kappa$ are arbitrary positive constants and α_m is a small threshold value. Using the adaptation law given in (12), the super-twisting SMC law in (11) is enhanced.

Theorem 1. Consider the nonlinear system in (4) and the sliding manifolds (8)–(9). There exist a range of arbitrary positive constants w_1, γ_1, ζ, η, κ and a finite time $T_1 > 0$ such that the sliding manifolds converge to the domain $|s| \leq \zeta$ in finite time if the control law is designed with the adaptive gains given by (12).

Proof 1. Initially, it is assumed that $x_1 \neq 0$, $x_3 \neq 0$ and also $s_1 \neq 0$, $s_2 \neq 0$. Taking Assumption 1 into account and calculating $\dot{s}$, we have

$$\dot{s} = -\alpha|s|^{\frac{1}{2}}\mathrm{sgn}(s) + \upsilon + d(t) \qquad \dot{\upsilon} = -\frac{\beta}{2}\mathrm{sgn}(s) \tag{13}$$

in which $d(t)$ is the total disturbance of the system.[14]

In order to carry out the Lyapunov analysis, a new state vector is defined as follows[9]

$$z = \begin{bmatrix} z_1 & z_2 \end{bmatrix}^T = \begin{bmatrix} |s|^{\frac{1}{2}}\mathrm{sgn}(s) & \upsilon \end{bmatrix}^T \tag{14}$$

Equation (14) can be rewritten as below

$$\dot{z}_1 = \frac{1}{2|z_1|}(-\alpha z_1 + z_2 + d(t)) \qquad \dot{z}_2 = -\frac{\beta}{|z_1|}\ z_1 \tag{15}$$

Referring to Assumption 1 and taking (7) into account, following inequality can be written

$$|d(t)| \leq \varsigma_0\sqrt{|s|} \tag{16}$$

where ς_0 is a positive and unknown constant. It can now be derived that

$$|d(t)| = \varsigma(x,t)\sqrt{|s|}\ \ \mathrm{sgn}(s) = \varsigma(x,t)\ \ z_1 \tag{17}$$

where $\varsigma(x,t)$ is a bounded function and $0 < \varsigma(x,t) \leq \varsigma_0$.

The system given in (15) is rewritten as below

$$\begin{bmatrix} \dot{z}_1 \\ \dot{z}_2 \end{bmatrix} = A\begin{bmatrix} z_1 \\ z_2 \end{bmatrix} \tag{18}$$

where

$$A := \frac{1}{2|z_1|}\begin{bmatrix} -\alpha + d(t) & 1 \\ -\beta & 0 \end{bmatrix} \tag{19}$$

According to this discussion, two cases can be observed. In the first case, $|z_1| = |s|^{1/2}$ and $\mathrm{sgn}(z_1) = \mathrm{sgn}(s)$. In the second case, if $z_1, z_2 \to 0$, then $s, \dot{s} \to 0$ in finite time.[9]

We choose the following Lyapunov function candidate

$$V = V_0 + \frac{1}{2\gamma_1}(\alpha - \alpha^*)^2 + \frac{1}{2\gamma_2}(\beta - \beta^*)^2 \tag{20}$$

in which γ_1 and γ_2 are positive constants. Besides, the adaptive gains are bounded and the unknown bounds of the adaptive gains are expressed as $\alpha^* > 0$ and $\beta^* > 0$. In (20), V_0 is defined as below

$$V_0 := (\lambda + 4\varepsilon^2)z_1^2 + z_2^2 - 4\varepsilon z_1 z_2 = z^T P z \tag{21}$$

with

$$P := \begin{bmatrix} \lambda + 4\varepsilon^2 & -2\varepsilon \\ -2\varepsilon & 1 \end{bmatrix} \tag{22}$$

where ε is a real number and $\lambda > 0$.

Time derivative of the Lyapunov function in (20) is given below

$$\dot{V} = \dot{V}_0 + \frac{1}{\gamma_1}(\alpha - \alpha^*)\dot{\alpha} + \frac{1}{\gamma_2}(\beta - \beta^*)\dot{\beta} \tag{23}$$

Taking (18)–(19) into account, we have

$$\dot{V}_0 = \dot{z}^T P z + z^T P \dot{z} \leq -\frac{1}{2|z_1|}z^T Q z \tag{24}$$

The symmetric matrix, Q, is computed as follows

$$Q = \begin{bmatrix} Q_{11} & Q_{12} \\ Q_{21} & 4\varepsilon \end{bmatrix} \tag{25}$$

where

$$Q_{11} = 2\lambda\alpha + 4\varepsilon(2\varepsilon\alpha - \beta) + 4\varepsilon\rho(x,t)$$
$$Q_{12} = Q_{21} = \beta - 2\varepsilon\alpha - \lambda - 4\varepsilon^2 - \rho(x,t)$$

We enforce $\beta = 2\varepsilon\alpha$ to guarantee the positive definiteness of the matrix Q and then Q will be positive definite with minimum eigenvalue $\lambda_{\min}(Q) \geq 2\varepsilon$ if the following condition holds true

$$\alpha > -\frac{\varepsilon(4\delta + 1)}{\lambda} + \frac{(2\delta + \lambda + 4\varepsilon^2)^2}{12\varepsilon\lambda} \tag{26}$$

As a result, the following inequality is obtained

$$\dot{V}_0 \leq -\frac{\varepsilon\lambda_{\min}^{1/2}(P)}{\lambda_{\max}(P)}V_0^{1/2} \tag{27}$$

According to (27), we can rewrite (23) and (24) as follows

$$\begin{aligned}\dot{V} &= \dot{z}^T P z + z^T P \dot{z} + \frac{1}{\gamma_1}(\alpha-\alpha^*)\dot{\alpha} + \frac{1}{\gamma_2}(\beta-\beta^*)\dot{\beta} \\ &\le -\frac{1}{|z_1|} z^T Q z + \frac{1}{\gamma_1}(\alpha-\alpha^*)\dot{\alpha} + \frac{1}{\gamma_2}(\beta-\beta^*)\dot{\beta} \\ &\le -\frac{\varepsilon\lambda_{\min}^{1/2}(P)}{\lambda_{\max}(P)} V_0^{1/2} - \frac{\omega_1}{\sqrt{2\gamma_1}}|\alpha-\alpha^*| \\ &\quad -\frac{\omega_2}{\sqrt{2\gamma_2}}|\beta-\beta^*| - |\alpha-\alpha^*|\left(\frac{1}{\gamma_1}\dot{\alpha} - \frac{\omega_1}{\sqrt{2\gamma_1}}\right) \\ &\quad -|\beta-\beta^*|\left(\frac{1}{\gamma_2}\dot{\beta} - \frac{\omega_2}{\sqrt{2\gamma_2}}\right)\end{aligned} \tag{28}$$

Taking Lemma 1 into account, the following inequality is obtained

$$\begin{aligned}-\frac{\varepsilon\lambda_{\min}^{1/2}(P)}{\lambda_{\max}(P)} V_0^{1/2} - \frac{\omega_1}{\sqrt{2\gamma_1}}|\alpha-\alpha^*| - \frac{\omega_2}{\sqrt{2\gamma_2}}|\beta-\beta^*| \\ \le -\eta_0\sqrt{V}\end{aligned} \tag{29}$$

where $\eta_0 = \min(\varepsilon\lambda_{\min}^{1/2}(P)/\lambda_{\max}(P)V_0^{1/2}, \omega_1, \omega_2)$. Then (28) can be rewritten as

$$\begin{aligned}\dot{V} \le -\eta_0\sqrt{V} - |\alpha-\alpha^*|\left(\frac{1}{\gamma_1}\dot{\alpha} - \frac{\omega_1}{\sqrt{2\gamma_1}}\right) \\ -|\beta-\beta^*|\left(\frac{1}{\gamma_2}\dot{\beta} - \frac{\omega_2}{\sqrt{2\gamma_2}}\right)\end{aligned} \tag{30}$$

Equation (30) can be written as in

$$\dot{V} \le -\eta_0\sqrt{V} + \xi \tag{31}$$

where

$$\begin{aligned}\xi := -|\alpha-\alpha^*|\left(\frac{1}{\gamma_1}\dot{\alpha} - \frac{\omega_1}{\sqrt{2\gamma_1}}\right) \\ -|\beta-\beta^*|\left(\frac{1}{\gamma_2}\dot{\beta} - \frac{\omega_2}{\sqrt{2\gamma_2}}\right)\end{aligned}$$

To show the finite time convergence, ξ can be vanished by using the following adaptation laws for α and β

$$\begin{aligned}\dot{\alpha} &= \omega_1\sqrt{\frac{\gamma_1}{2}} \\ \dot{\beta} &= \omega_2\sqrt{\frac{\gamma_2}{2}}\end{aligned} \tag{32}$$

With these selections, we have $\xi = 0$ and

$$\dot{V} \le -\eta_0\sqrt{V} \tag{33}$$

According to Lemma 2, there exists a finite time $T_1 > 0$, for $t \ge T_1$ and the sliding variable s enters the domain $|s| \le \zeta$

$$T_1 \le T_0 + \frac{2V^{1/2}(T_0)}{\eta_0} \tag{34}$$

where $\eta_0 = \min(r, \omega_1, \omega_2)$ and T_0 denotes the initial time.

Theorem 2. The switching variable s enters the domain $|s| \le \zeta$ in finite time and it may violate this inequality for finite time intervals. However, there always exists a larger domain called W to which $|s|$ belongs

$$W := \left\{s, \dot{s} : |s| \le \eta_1, \left|\dot{s}\right| \le \eta_2, \eta_1 > \zeta\right\} \tag{35}$$

where $\eta_1 > 0$ and $\eta_2 > 0$ are some boundary parameters.

Proof 2. Suppose that $|s| \le \zeta$ for α given by (12). This leads to the following

$$\dot{\alpha} = \begin{cases} -w_1\sqrt{\gamma/2} & : \alpha \ge \alpha_m \\ \eta & : \alpha < \alpha_m \end{cases} \tag{36}$$

If α is less than α_m, its value immediately starts to increase such that $\alpha = \alpha_m + \eta t$. When the system states satisfy $|s| \le \zeta$, the control gains α and β will decline gradually. Afterwards, the system states may deviate from the domain $|s| \le \zeta$ because of the decrease of the gains α and β. In this case, α and β will gradually increase thanks to the effect of the adaptive law and the sliding variable s enters the domain, which is $|s| \le \zeta$, in finite time.[26,27] Accordingly, it can be assured that $|s| \le \eta_1, \eta_1 > \zeta$,.[14] Moreover, when $|s| \le \zeta$, the first derivative of the sliding variable value $|\dot{s}|$ satisfies the inequality given below

$$|\dot{s}| \le \alpha\zeta^{\frac{1}{2}} + (\varepsilon\alpha + \zeta)(T_2 - T_1) := \overline{\eta}_2 \tag{37}$$

where T_1 is the time instant when s enters the domain $|s| \le \zeta$ and T_2 is the time instant when s leaves this domain,[14]

There is a final case $\zeta < |s| \le \eta_1$, which needs to be studied

$$\begin{aligned}|\dot{s}| \le \left(\eta_1^{\frac{1}{2}} + \varepsilon\right)\left(\alpha + \omega_1\sqrt{\frac{\eta_1\gamma_1}{2}}\right)(T_3 - T_2) \quad + \zeta(T_3 - T_2) \\ := \tilde{\eta}_2\end{aligned} \tag{38}$$

where T_2 is the time instant when s leaves the domain $|s| \le \zeta$ and T_3 is the time instant when s enters this domain afterwards. When the conditions given in (37) and (38) are taken into consideration, the following inequality can be written

$$|s| \le \max\left(\overline{\eta}_2, \tilde{\eta}_2\right) := \eta_2 \tag{39}$$

As a result, considering the above inequality, the switching variable s is guaranteed to stay always in a larger domain and the sliding regime is established for α and β given by 31.

Adaptive super-twisting sliding mode guidance law design with fuzzy logic system

In this subsection, a novel guidance law is designed based on the aforementioned super-twisting sliding mode control, adaptive algorithm, and a fuzzy gain scheduler. The super-twisting sliding mode control and the adaptive

algorithm are described in detail and designed in the previous section. Moreover, the parameters k_1, k_2 of the sliding manifold given in (8)–(9) are unknown constants and the fuzzy logic system is used for the selection of gains. Various uncertainty problems may arise in determining these gains manually as determining these gains is difficult and complicated and additionally the process requires experience. In Figure 2, the block diagram of the adaptive super-twisting sliding mode guidance law design with the fuzzy logic system is illustrated.

A fuzzy logic system consists of four fundamental units, namely, fuzzifier, inference engine, rule base, and defuzzifier, respectively. Figure 3 shows a general fuzzy logic system structure and the details are given in the sequel.

Selection of the fuzzy logic system inputs and outputs. There are two independent fuzzy modules in the design of the proposed guidance law. The elevation LOS angle and its time derivative $(\theta, \dot{\theta})$ are introduced as the input to the first fuzzy module and the azimuth LOS angle and its rate $(\phi, \dot{\phi})$ are introduced as the input to the second module. The output of each fuzzy module provides control gains k_1 and k_2 given in (8) and (9), respectively.

Membership functions. Triangular Membership Functions (MFs) are used with linguistic labels N, Z, and p denoting negative, zero, and positive, respectively, for the input variables and S, M, B, which stand for small, medium, and big, are used for the output variable. The MFs used in this study are shown in Figure 4.

Fuzzy rule base. jth fuzzy rules for ϕ and θ subsystems are given as

$$Rule\#j: \text{IF } \phi \text{ is } \mathrm{F}_1^{l_1} \text{ and } \dot{\phi} \text{ is } \mathrm{F}_2^{l_2} \text{ THEN } k_1 \text{ is } B^j$$

$$Rule\#j: \text{IF } \theta \text{ is } \mathrm{F}_1^{l_1} \text{ and } \dot{\theta} \text{ is } \mathrm{F}_2^{l_2} \text{ THEN } k_2 \text{ is } B^j$$

where $l_i = 1, 2, 3$, $i = 1, 2$, $j = 1, 2, \ldots, 9$ and B^j is the fuzzy output of the jth fuzzy rule. Table 1 presents the lingustic descriptions used in the fuzzy modules.

Defuzzifier. In this study, we utilize centroid deffuzzifier with the output MFs shown in Figure 4.

The very role of the fuzzy modules is to provide appropriate gains as described in the rule tables shown above. This prevents using unnecessarily large gains for the fuzzy subspaces where small values are needed.

Simulation and analysis

In this section, numerical simulations are studied for three different scenarios to prove the merits and effectiveness of the proposed guidance law, which is compared with the aforementioned guidance laws.

The initial conditions of the presented guidance system are selected as follows. The initial velocity of the missile is V_{M0} = 800 m/s and the initial position of the missile is x_{M0} = 0 m, y_{M0} = 5000 m, and z_{M0} = 0 m. The initial velocity of the target is V_{T0} = 300 m/s and the initial position of the target is x_{T0} = 2500 m, y_{T0} = 4000 m, and z_{T0} = 200 m. In addition to these, the initial flight-path angle of the missile is $\phi_{M0} = 0°$ and the heading angle of the missile is $\theta_{M0} = 8°$. For the target, the initial flight-path angle is $\phi_{T0} = 0°$, and the heading angle is $\theta_{T0} = 8°$. g = 9.81 m/s^2 is the gravitational constant.

To verify the performance of the proposed guidance laws, these guidance laws are compared with the SM guidance law in.[28] Thus, the obtained results from four different guidance laws are given in this article and these are SM, STWSM, ASTWSM, and AFSTWSM guidance law.

Table 2 gives three different scenarios that describe target accelerations and different disturbance levels.[29,30] These scenarios will be used to show the effectiveness and robustness of the presented guidance laws. Besides, the simulations are carried out in the presence of external

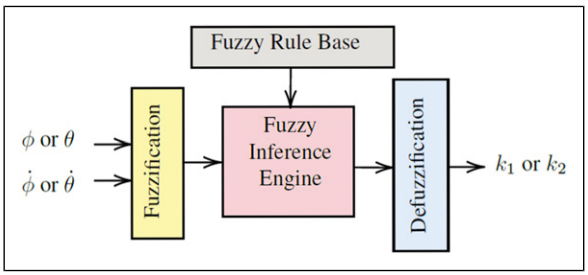

Figure 3. General fuzzy logic system structure with input/output quantities $(\phi, \dot{\phi}) \rightarrow k_1$ and $(\theta, \dot{\theta}) \rightarrow k_2$.

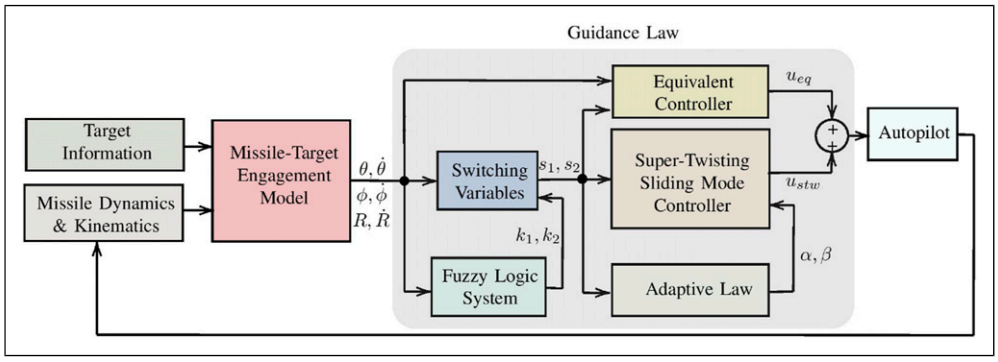

Figure 2. The block diagram of the ASTWSM with fuzzy logic system guidance law.

disturbances in order to assess the performance of the guidance laws fairly.

Case 1. Non-maneuvering target

In Case 1, the goal of the missile is to intercept the target, which is non-maneuvering. The parameters of the sliding variables (8)–(9) are chosen as $k_1 = 0.03$, $k_2 = 0.0025$ for using in the STWSM guidance law. The parameters of the STWSM guidance law (11) are selected as $\alpha = 0.007$ and $\beta = 0.012$. Further to these, $\omega_1 = 2$, $\gamma = 0.02$, $\zeta = 0.06$, $\eta = 0.02$, $\kappa = 0.01$, and $\alpha_m = 0.005$ are chosen to use in the developed ASTWSM guidance law and the proposed AFSTWSM guidance law.

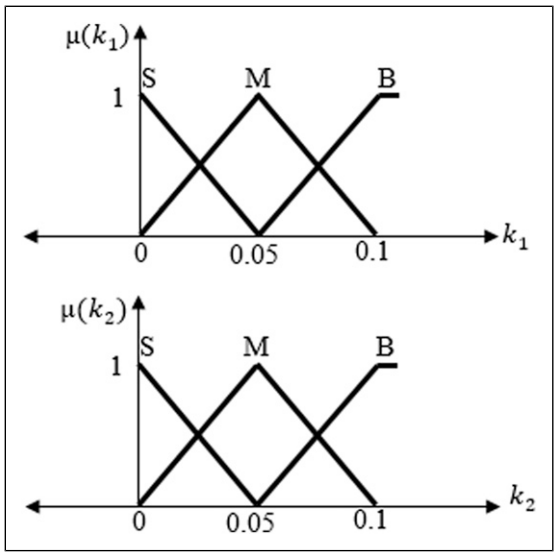

Figure 4. Membership function of linguistic variables for the outputs k_1, k_2.

Table 1. Two dimensional fuzzy rule bases.

$\theta/\dot{\theta}$	**N**	**Z**	P
N	S	S	M
Z	S	M	B
p	M	B	B
$\phi/\dot{\phi}$	**N**	**Z**	P
N	S	S	M
Z	S	M	B
p	M	B	B

For Case 1, the final miss distance and the time of interception are tabulated in Table 3. The earliest interception time and small miss distance are the most important criteria in the missile-target interception system. According to these criteria, it can be seen from the results given in Table 3 that both ASTWSM and AFSTWSM guidance laws have the smallest miss distance compared to other guidance laws. Also, the AFSTWSM guidance law hits the target in a shorter time than the other guidance laws. In addition, the final closing velocity values are presented in the table.

The relative distance r, the missile-target interception, the response of LOS angle and LOS angular rate, phase space behavior of the elevation angle s_1 and $\dot{s}_1$, phase space behavior of the azimuth angle s_2 and $\dot{s}_2$, and the missile's accelerations are demonstrated in the subplots of Figure 5, respectively. It can be clearly seen from in Figure 5(a) that the relative range decreases to zero at the intercept time in all of the guidance laws. Thus, the missile with these guidance laws successfully hits the target in this case. In Figure 5(b), the missile's and target's trajectories guided by guidance law is given. Figure 5(c) demonstrates the response of the LOS angles. Figure 5(d) demonstrates the response of the LOS angular rates. Figures 5(e) and (f) show the controlled phase space behavior of the switching manifold defined for the elevation angle and the azimuth angle, respectively. The missile's accelerations are given in Figure 5(g).

Case 2. Time-varying maneuvering target

In Case 2, the target has a maneuvering trajectory and the missile aims to intercept this target. The parameters of the switching variables in (8)–(9) are set as $k_1 = 0.021$, $k_2 = 0.022$ for the STWSM guidance law. Moreover, the parameters of the

Table 2. Accelerations of target and levels of disturbance in interception scenarios.

Interception scenarios	Azimuth acceleration	Elevation acceleration	Disturbance
Non-maneuvering	g	0	Chirp signal
Time-varying maneuvering	$3g + \sin 2\pi t$	$3g + \sin 2\pi t$	Chirp signal
Time-varying maneuvering with different disturbance level	$3g + \sin 2\pi t$	$3g + \sin 2\pi t$	Band-limited white noise

Table 3. Miss distance, interception time, and final closing velocity for Case 1.

Guidance law	Miss distance (m)	Interception time (s)	Final closing velocity (m/s)
SMGL	0.4043	4.501	584.06
STWSMGL	0.4103	4.499	585.69
ASTWSMGL	0.2471	4.499	604.35
AFSTWSMGL	0.1551	4.498	608.55

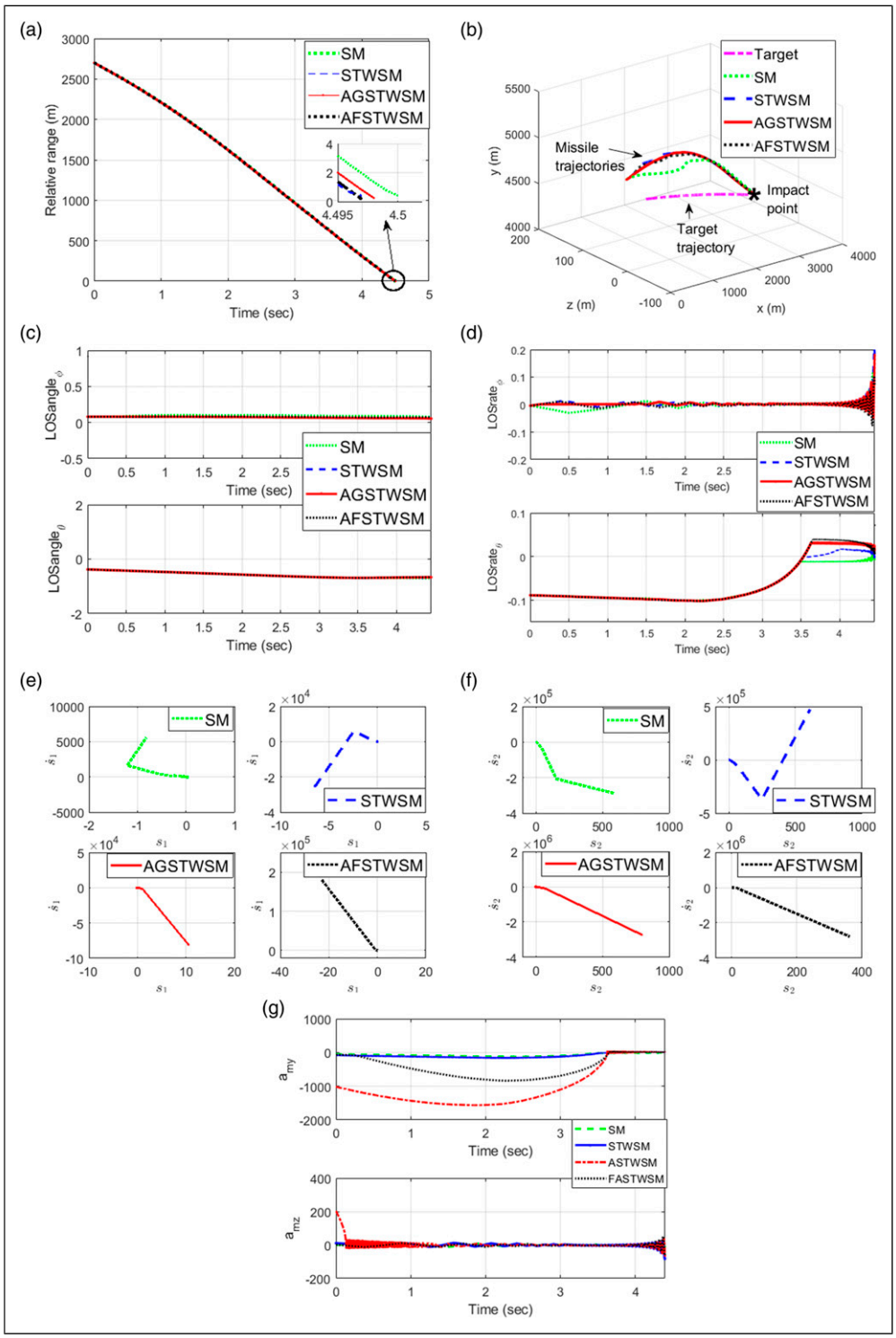

Figure 5. Results of Case 1 (a) Relative range; (b) Missile and Target trajectories; (c) LOS angles; (d) LOS angular rates; (e) Phase space behavior of the elevation angle; (f) Phase space behavior of the azimuth angle; (g) Missile's accelerations.

STWSM guidance law (11) are selected as $\alpha = 0.002$ and $\beta = 0.05$. We chose $\omega_1 = 2, \gamma = 0.2, \zeta = 0.05, \eta = 0.02, \kappa = 0.01$, and $\alpha_m = 0.005$ for the ASTWSM and AFSTWSM guidance laws.

For Case 2, Table 4 summarizes the comparison of the interception performances of the four guidance laws by giving the final time, the miss distance and the final closing velocity. According to the tabulated results, we can infer that the miss distance arising under the proposed AFSTWSM guidance law is smaller than the distances in other alternatives. Also, the proposed AFSTWSM guidance approach is one of the best performing approaches among the given guidance laws for the interception time. Moreover, the final closing velocity values are given in the table.

The observed variables in this case are illustrated in Figure 6, respectively. In Figure 6(a), the relative range

Table 4. Miss distance, interception time, and final closing velocity for Case 2.

Guidance law	Miss distance (m)	Interception time (s)	Final closing velocity (m/s)
SMGL	0.4072	4.237	653.63
STWSMGL	0.1291	4.234	647.63
ASTWSMGL	0.2508	4.232	676.44
AFSTWSMGL	0.2434	4.229	679.14

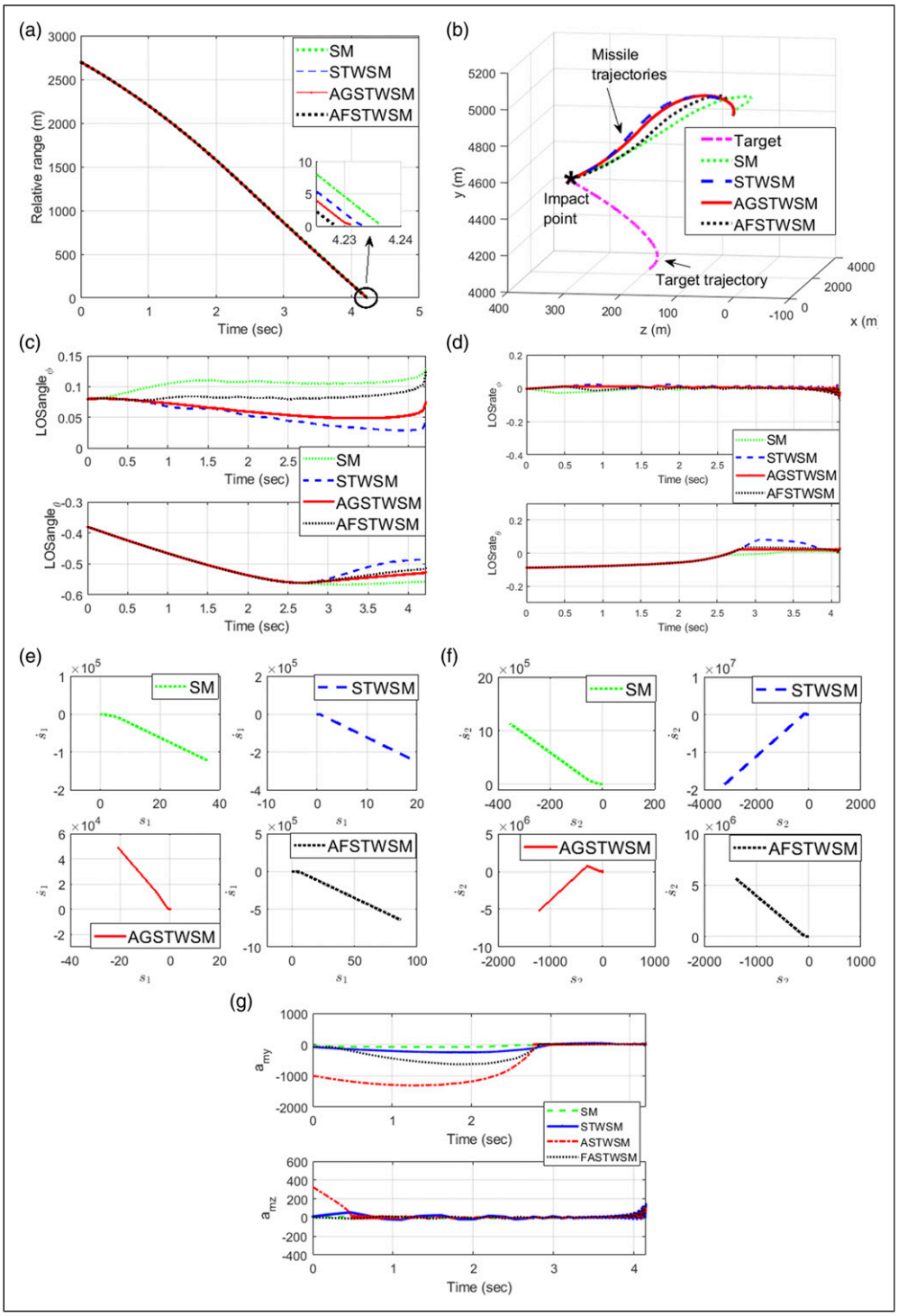

Figure 6. Results of Case 2 (a) Relative range; (b) Missile and Target trajectories; (c) LOS angles; (d) LOS angular rates; (e) Phase space behavior of the elevation angle; (f) Phase space behavior of the azimuth angle; (g) Missile's accelerations.

Table 5. Miss distance, interception time, and final closing velocity for Case 3.

Guidance law	Miss distance (m)	Interception time (s)	Final closing velocity (m/s)
SMGL	0.4999	4.240	609.04
STWSMGL	0.3752	4.234	632.36
ASTWSMGL	0.3267	4.234	656.72
AFSTWSMGL	0.1515	4.229	669.89

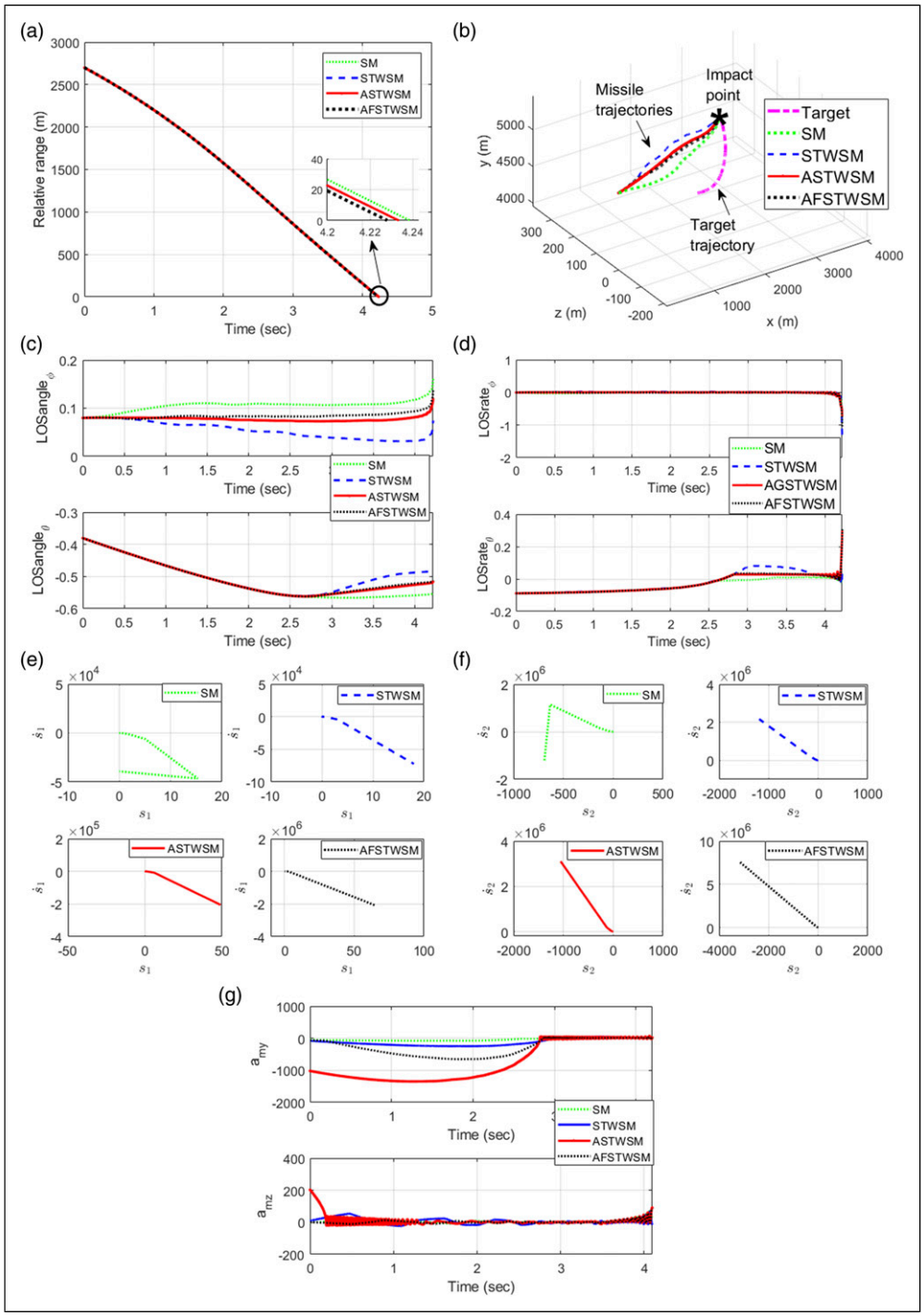

Figure 7. Results of Case 3 (a) Relative range; (b) Missile and Target trajectories; (c) LOS angles; (d) LOS angular rates; (e) Phase space behavior of the elevation angle; (f) Phase space behavior of the azimuth angle; (g) Missile's accelerations.

decreases to zero at the interception time in all of the guidance laws, that is, the missile with the studied guidance laws successfully hits the target in this case. The trajectories of the missile and the target, guided by the law of guidance, are given in Figure 6(b). Figure 6(c) shows the response of the LOS angles. Figure 6(d) gives the response of the LOS angular rates. Figures 6(e) and (f) present the controlled phase space behavior of the switching manifold defined for the elevation angle and the azimuth angle. The missile's accelerations are shown in Figure 6(g). The observations in Figure 6 suggest that the missile hits the target accurately for all guidance laws yet the proposed adaptive and fuzzy-enhanced adaptive schemes display prominent features.

Case 3. Time-varying maneuvering target with different disturbance level

In Case 3, the target has a maneuvering trajectory and the external disturbance is chosen from the different disturbance levels. This disturbance is the band-limited white noise. And under these conditions, the missile aims to intercept this target. The parameters of the switching variables in (8)–(9) are set as $k_1 = 0.021$, $k_2 = 0.022$ for the STWSM guidance law. Moreover, the parameters of the STWSM guidance law (11) are selected as $\alpha = 0.002$ and $\beta = 0.05$. We chose $\omega_1 = 2$, $\gamma = 0.2$, $\zeta = 0.05$, $\eta = 0.02$, $\kappa = 0.01$, and $\alpha_m = 0.006$ for the ASTWSM and AFSTWSM guidance laws.

For Case 3, Table 5 summarizes the comparison of the interception performances of the four guidance laws by giving the final time, the miss distance, and the final closing velocity. According to the presented results, we can infer that the miss distance arising under the proposed AFSTWSM guidance law is smaller than the distances in other alternatives. Also, the proposed AFSTWSM guidance approach is one of the best performing approaches among the given guidance laws for the interception time. Lastly, the final closing velocity values are presented in the table.

The observed variables in this case are illustrated in Figure 7, respectively. In Figure 7(a), the relative range decreases to zero at the interception time in all of the guidance laws, that is, the missile with the studied guidance laws successfully hits the target in this case. The trajectories of the missile and the target, guided by the law of guidance, are given in Figure 7(b). Figure 7(c) shows the response of the LOS angles. The response of the LOS angular rates is given in Figure 7(d). Figures 7(e) and (f) present the controlled phase space behavior of the switching manifold defined for the elevation angle and the azimuth angle. In Figure 7(g), the missile's accelerations are demonstrated. The observations in Figure 7 suggest that the missile hits the target accurately for all guidance laws yet the proposed adaptive and fuzzy-enhanced adaptive schemes display prominent features.

Conclusions

In this paper, a new adaptive super-twisting sliding mode guidance law with a fuzzy gain scheduling is proposed for the missile-target interception. The super-twisting sliding mode guidance law is chosen to eliminate the chattering phenomenon. A novel adaptive law is used to obtain the controller gains without entailing the upper bound of the disturbance. The control system is augmented with a fuzzy inference system to prevent overestimation of the unknown parameters of the controller. A set of simulation scenarios is studied for the four guidance laws, which are the traditional SM guidance law, the traditional STWSM guidance law, the proposed ASTWSM guidance law, and the proposed AFSTWSM guidance law. The obtained results demonstrate that the proposed adaptive and fuzzy-enhanced adaptive approaches have better performances in terms of the intercept time, the miss distance, and the final closing velocity compared to the traditional alternatives.

Declaration of conflicting interests

The author(s) declared no potential conflicts of interest with respect to the research, authorship, and/or publication of this article.

Funding

The author(s) disclosed receipt of the following financial support for the research, authorship, and/or publication of this article: Handan Gürsoy-Demir was supported by The Scientific and Technological Research Council of Turkey (TÜBİTAK-BİDEB) with PhD scholarship 2211-C (the encouragement scholarship for priority areas). This work is a part of Handan Gürsoy-Demir's PhD dissertation.

ORCID iD

Handan Gürsoy-Demir https://orcid.org/0000-0001-5486-454X

References

1. Zhang Y, Sun M and Chen Z. Finite-time convergent guidance law with impact angle constraint based on sliding-mode control. *Nonlinear Dyn* 2012; 70(1): 619–625.
2. Pushpangathan JV, Kandath H and Balakrishnan A. Hit-to-kill accurate minimum time continuous second-order sliding mode guidance for worst-case target maneuvers. *Proc. Inst. Mech. Eng. G: J. Aerosp. Eng* 2021; 235(7): 729–744.
3. Shin HS, Tsourdos A and Li KB. A new three-dimensional sliding mode guidance law variation with finite time convergence. *IEEE Trans Aerosp Electron Syst* 2017; 53(5): 2221–2232.
4. Geng ST, Zhang J and Sun JG. Adaptive back-stepping sliding mode guidance laws with autopilot dynamics and acceleration saturation consideration. *Proc. Inst. Mech. Eng. G: J. Aerosp. Eng* 2019; 233(13): 4853–4863.
5. Li C, Wang J, He S, et al. Collision-geometry-based generalized optimal impact angle guidance for various missile and target motions. *Aerosp Sci Technol* 2020; 106: 106204.
6. Savkin AV, Pathirana PN and Faruqi FA. Problem of precision missile guidance: LQR and H//sup∞/control frameworks. *IEEE Trans Aerosp Electron Syst* 2003; 39(3): 901–910.
7. Zhao H, Wang M, Zhang X, et al. A high-order sliding mode variable structure guidance law with finite time convergence. In: Proceedings of the 2016 IEEE advanced information management, communicates, electronic and automation control conference (IMCEC). Xi'an, China, 03–05 October 2016, pp. 641–647.

8. Wang Z. Adaptive smooth second-order sliding mode control method with application to missile guidance. *Trans. Inst. Meas. Control* 2017; 39(6): 848–860.
9. Shtessel YB, Moreno JA, Plestan F, et al. *Super-twisting adaptive sliding mode control: a lyapunov design*. In: Proceedings of the 49th IEEE conference on decision and control (CDC), Atlanta, Georgia, USA, 2007, pp. 5109–5113, IEEE.
10. Zhao Y, Huang P and Zhang F. Dynamic modeling and super-twisting sliding mode control for tethered space robot. *Acta Astronaut* 2018; 143: 310–321.
11. Jayakrishnan H. Position and attitude control of a quadrotor uav using super twisting sliding mode. *IFAC-PapersOnLine* 2016; 49(1): 284–289.
12. Yang F, Zhang K and Yu L. Adaptive super-twisting algorithm-based nonsingular terminal sliding mode guidance law. *J. Control Sci. Eng* 2020; 2020(2): 11–11.
13. Babaei AR, Malekzadeh M and Madhkhan D. Adaptive super-twisting sliding mode control of 6-dof nonlinear and uncertain air vehicle. *Aerosp Sci Technol* 2019; 84: 361–374.
14. Li G and Wu Y. Nonsingular adaptive-gain super-twisting guidance with an impact angle constraint. *Proc. Inst. Mech. Eng. G: J. Aerosp. Eng* 2019; 233(5): 1705–1714.
15. Feng Z and Fei J. Design and analysis of adaptive super-twisting sliding mode control for a microgyroscope. *PloS one* 2018; 13(1): e0189457.
16. Yang Y and Yan Y. Attitude regulation for unmanned quadrotors using adaptive fuzzy gain-scheduling sliding mode control. *Aerosp Sci Technol* 2016; 54: 208–217.
17. Goel A and Swarup A. Adaptive fuzzy high-order super-twisting sliding mode controller for uncertain robotic manipulator. *J. Intell Sys* 2017; 26(4): 697–715.
18. Liu E, Yang Y and Yan Y. Spacecraft attitude tracking for space debris removal using adaptive fuzzy sliding mode control. *Aerosp Sci Technol* 2020; 107: 106310.
19. Xu S, Gao M, Fang D, et al. A novel adaptive second-order nonsingular terminal sliding mode guidance law design. *Proc. Inst. Mech. Eng. G: J. Aerosp. Eng* 2020; 234(16): 2263–2273.
20. Li Q, Zhang W, Han G, et al. Fuzzy sliding mode control guidance law with terminal impact angle and acceleration constraints. *J of Syst Eng Electron* 2016; 27(3): 664–679.
21. Elhalwagy YZ and Tarbouchi M. Fuzzy logic sliding mode control for command guidance law design. *ISA Trans* 2004; 43(2): 231–242.
22. Guo J, Li Y and Zhou J. A new continuous adaptive finite time guidance law against highly maneuvering targets. *Aerosp Sci Technol* 2019; 85: 40–47.
23. Chen Z, Chen W, Liu X, et al. Three-dimensional fixed-time robust cooperative guidance law for simultaneous attack with impact angle constraint. *Aerosp Sci Technol* 2021; 110: 106523.
24. Hardy GH, Littlewood JE and Pólya G. *Inequalities*. Cambridge, UK: Cambridge University Press, 1952.
25. Liu X and Li G. Adaptive sliding mode guidance with impact time and angle constraints. *IEEE Access* 2020; 8: 26926–26932.
26. Lee SD, Hong Phuc BD, Xu X, et al. Roll suppression of marine vessels using adaptive super-twisting sliding mode control synthesis. *Ocean Eng* 2020; 195: 106724.
27. Dong Q, Zong Q, Tian B, et al. Adaptive-gain multivariable super-twisting sliding mode control for reentry rlv with torque perturbation. *Int J Robust Nonlinear Control* 2017; 27(4): 620–638.
28. Gürsoy-Demir H and Efe MÖ. Comparison of three-dimensional guidance laws for missile guidance system. In: 10th Ankara international aerospace conference, Ankara, TurkeyMETU, 1–13, 2019.
29. Zhang K and Yang S. Second-order sliding mode guidance law considering second-order dynamics of autopilot. *J. Control Sci. Eng* 2019; 2019: 1–11.
30. Kumar SR, Rao S and Ghose D. Sliding-mode guidance and control for all-aspect interceptors with terminal angle constraints. *J. Guid. Control Dyn* 2012; 35: 1230–1246.

Appendix

Nomenclature

a_{MR} Component of the missile acceleration
$a_{M\theta}$ Component of the missile acceleration
$a_{M\phi}$ Component of the missile acceleration
a_{TR} Component of the target acceleration
$a_{T\theta}$ Component of the target acceleration
$a_{T\phi}$ Component of the target acceleration
$d(t)$ Total disturbance
R Relative distance
$\dot{R}$ Relative velocity
s Vector of the sliding manifolds
u_{eq} Equivalent control
u_{stw} Super-twisting control
θ The elevation angle
ϕ The azimuth angle
α, β The controller gains
α_m A small threshold value